Angle dependent quality factor of Mie resonances in silicon colloids based microcavities

Journal:	*ACS Photonics*
Manuscript ID:	ph-2013-00134t
Manuscript Type:	Article
Date Submitted by the Author:	22-Nov-2013
Complete List of Authors:	Shi, Lei; Universidad Politecnica de Valencia, Centro de Tecnologias Fisicas, Unidad Asociada ICMM/CSIC-UPV Fenollosa, Roberto; CSIC, Tuzer, T. Umut; CSIC, Meseguer, Francisco; CONSEJO SUPERIOR DE INVESTIGACIONES CIENTIFICAS, UNIDAD ASOCIADA CSIC-UPV

Angle dependent quality factor of Mie resonances in silicon colloids based microcavities

Lei Shi*, Roberto Fenollosa, T. Umut Tuzer and Francisco Meseguer
Centro de Tecnologias Fisicas,
Unidad Asociada ICMM/CSIC-UPV,
Universidad Politecnica de Valencia,
Av. Los Naranjos s/n, Valencia, 46022 (Spain)
Instituto de Ciencia de Materiales de Madrid CSIC
Madrid, 28049, (Spain)
E-mail: shilei@upv.es

Abstract:
Semiconductor photonic microcavities are very important elements in the field of photonics nowadays. The light trapping ability of 3D silicon spherical micrometer size photonic cavities, which are fabricated by easy chemical methods, as well as the quality factor measurement, is here reported. We have shown through both experiments and theoretical modelisations that the observed quality factor of the modes of a spherical silicon microcavity located on a dielectric substrate can be easily tuned by only changing the incident angle of the light. This special angle dependent property could be used to design high efficiency angle resolved photo-detectors and micrometric size optoelectronic power source devices.

Keyword

Semiconductor Photonic Cavity, Silicon Colloids, Quality factor, Mie resonance

Semiconductor photonic cavities (SPCs) are one of the most important optical components in today's technology. Their ability to confine light in a small volume,[1] and the enormous optoelectronic applications developed so far[2] have raised them as key elements for the near future technological developments. Many types of SPCs, such as one or two dimensional (2D) photonic crystal cavities[3, 4] and micro-disk cavities[5, 6] have been reported. They can trap light very efficiently, and can be easily integrated into photonic micro-circuitry. On the other hand, three dimensional (3D) SPCs, such as spherical cavities, have been much less researched because of their

intrinsic fabrication difficulties. Recently, some of us have reported on silicon spherical nano[7] and micro[8] cavities fabricated through chemical vapor deposition (CVD) techniques. The studies performed so far have been concentrated on the cavity performance of these silicon colloids based SPCs,[7-9] as well as on the applications to different types of devices.[10, 11, 12] Normally, at difference to 2D SPCs where light is coupled into the cavity via the near field, such as the evanescent field of the waveguide, silicon colloid based 3D SPCs are located on a certain substrate in such a way that the light couples into the cavity from the far field. Because the resonance plane of the 3D cavity touches the substrate at only one point, one could think that the influence of the substrate is negligible, especially for those substrates with low refractive index and therefore the Mie theory of isolated microcavities can account for experimental results. This hypothesis, however, has been never proved.

Here, through theoretical and experimental evidences, we show how the substrate influences substantially the optical properties of silicon colloid based SPCs. We analyze the influence of the substrate on the quality factor (Q) of the resonant modes. This is a key parameter for assessing the quality performance of a photonic cavity. The higher the Q, the longer the lifetime of the photons trapped inside the cavity, and the narrower is the resonance. However, higher Q value does not always mean a better device performance. High Q values[1, 3-5] are necessary in some research fields such as non-linear optics, and quantum information, etc.[13-15] In other applications, like those concerning luminescence emission enhancement of a lucent specie inside a cavity,[16,

[17] moderate values of the Q factor are necessary. Finally, in the case of cavity based photovoltaic devices, there is an optimized Q value, which depends on the absorption coefficient, for achieving the maximum absorption efficiency.[2, 18-20] Therefore, the study of the environmental factors influencing the Q factor of a cavity is very important, and they can provide new ideas about tuning this parameter in a controlled way. In this paper, we show how the observed Q factor value of a silicon colloid based SPC can be easily modified by changing the direction of the incident light. This angle dependant property could help us finding the optimized Q value for realizing devices like high efficiency angle resolved photodetectors and micrometer size optoelectronic power sources.[21, 22]

Silicon colloid based SPCs were fabricated by a Chemical Vapor Deposition (CVD) method, using disilane (Si_2H_6) as a precursor gas, as it has been described elsewhere (see also the experimental section).[8] It should be mentioned that, 1) the processing method is quick, cheap and compatible with industry silicon CVD fabrication process; 2) the silicon spherical cavities have a very tiny volume (diameters are about 2-3 micrometers shown here), and they have a high optical performance (shown below). Figure 1a shows the optical microscopy image of a typical silicon spherical SPC. The SEM image of the cavity is also shown in the figure inset. Through micromanipulation techniques, fabricated nanocavities were located on a glass substrate. We performed angle resolved optical transmission experiments on single particles with the help of a custom-made confocal microscope (details shown in the

Methods) attached to a spectrometer with an InGaAs detector.

Before showing the experimental and theoretical results of the angle resolved optical properties, we firstly discuss how the observed Q factor of different optical modes of a spherical silicon micro-cavity located on a substrate depends on the direction of the incident light. An isolated photonic cavity with a spherical shape should have isotropic optical properties, which are well described by the Mie theory, where all the Mie modes can be separated into two groups. The modes of the first one, labeled as "a" group, resonate in a plane that is parallel to the electric component of the incident light. The modes of the second one, labeled as "b" group, resonate in a plane that is perpendicular to the electric component of the incident light.[23] Whenever the spherical cavity is placed on a certain dielectric substrate, the isotropy of the Mie modes is destroyed and the Q factors of those degenerated-broken modes observed from the experiments could be strongly dependent on the incident angle of the light. This occurs specially for those modes whose resonant plane intersects with the substrate. Figure 1b shows the schematic view of an s-wave polarized light impinging on a spherical silicon SPC located on a substrate at certain incident angle ϕ, and also both resonance planes corresponding to "a" (yellow dash line), and "b" (red dash line) modes. Then it is easy to understand the influence of the light incident angle on the observed Q factors of the "a" and "b" modes separately. While the resonance plane of “b” modes (red dash line) intersects always at 90 degree with the substrate no matter the angle ϕ, the resonant plane of “a” modes (yellow dash line) intersects at 90 degree

with the substrate only for ϕ equal to zero. Therefore, one expects that in general the observed Q of “b” modes is, independently of ϕ,lower than that of the ideal case, when the sphere is isolated, and the observed Q of “a” modes to be variable with the incident angle of light, achieving higher values of Q as ϕ increases. In any case, the influence of the substrate will depend for each mode on its particular electromagnetic field distribution and its extension in the mode volume. For instance, Figure 1c and 1d show the electric field intensity distribution of modes $a_{11,6}$ and $b_{9,4}$ respectively in the two perpendicular planes defined by the dash yellow (left panels) and dash red (right panels) lines. One can see that both modes are distributed in all the spherical volume. However, for the $a_{11,6}$ mode, the electric field is much more concentrated in the yellow dash line plane, which should be the resonant plane for all the "a" modes, and for the $b_{9,4}$ mode, it is more concentrated in the red dash line plane, which should be the resonant plane for all the "b" modes. In the case of p-wave incidence, similar analyses can be easily repeated, with opposite results, i. e. in this case it is the observed Q of “b” modes that is expected to vary with ϕ. In summary, we expect that the experimental observed Q factor of both types of modes can be easily tuned by changing the k-vector of the incident light and by choosing the appropriate polarization. Obviously, for non-polarized light we expect the observed Q of all of the modes to become higher as the angle of the incident light increases. The scattering with non-polarized light occurs in many applications like those of micro or nano optoelectronic power sources and photon-detectors, and it will be studied here in detail.

Figure 2 shows the optical transmission experiments of spherical SPCs located on a glass substrate for three different diameter values: 3.310 μm (Figure 2a), 2.546 μm (Figure 2b) and 2.348 μm (Figure 2c). These values are the result of a fitting process which will be explained below. The transmission dips in each spectrum correspond to Mie resonances. The smaller the cavity the less Mie modes it can support in a finite range of measurement, and therefore the less transmission dips are observed. For all the cavities, we shined non-polarized light at different incident angles. The bottom black lines correspond to the normal incident case (ϕ=0). The blue, light blue, green and red lines correspond to 20, 40, 60 and 70 degrees of incidence respectively. For the ϕ=0 case, all transmission dips of all the cavities are broad, which indicates low Q values of the Mie modes. When the incident angle is gradually increased, most transmission dips get sharper and even new transmission dips appear. To clearly show these results, we zoom in the areas marked by an orange band in the spectra to the right panels of Figure 2. These panels indicate the position of three modes, namely $a_{12,5}$, $b_{9,4}$, $b_{10,4}$ by red, green and blue arrows respectively, whose Q variation with the incident angle will be studied more in detail in the Figure 4.

To deeper understand the experimental results, we performed theoretical simulations of the scattering efficiency of single spherical silicon SPCs located on a glass substrate at different values of the incidence angle by using the null-field method with discrete sources (details shown in Methods). In the calculation, we assumed a refractive index dispersion similar to that of silicon grown by Plasma Enhanced

Chemical Vapor Deposition [24] (see Methods). It allowed us fitting the experimental spectra to the theoretical simulations in all the measurement range by using the sphere diameter as the only fitting parameter. The refractive index of glass was considered to have a constant value of 1.45. Figure 3a shows the calculated scattering efficiency of the 3.310 μm diameter silicon SPC located on a glass substrate. Non-polarized light was used in the simulations to mimic the experimental setup. The different color spectra shown in the figure, from the bottom one (black spectrum) to the top one (red spectrum) correspond to different angles of incidence, namely ϕ=0º, 20º, 40º, 60º and 70º. The corresponding experimental transmission spectra (see Figure 2a) are also shown for each angle (purple curves) for confirming the good agreement between theory and experiment. The resonances obtained in experimental results appear here as peaks instead of dips because the transmission scales have been inverted. Similarly to the experiments, the calculated spectrum for normal incidence shows broad resonances. Also high Q values (narrow) peaks are missing. When the light incident angle increases, the peaks get sharper and their Q value increase. In the top panel of Figure 3a, the calculated spectrum of a silicon colloid SPC having the same diameter as that of the other spectra, i. e. 3.310 μm, but free standing in air is also shown (grey line). Clearly, this spectrum is similar to that of the cavity on glass for the incidence angle at ϕ=70º (red curve) within the resolution used in the simulation. Of course, discrepancies may arise for the highest Q resonances if such resolution is increased. On another hand, it should be mentioned that the spectrum of the free standing silicon colloid SPC has been multiplied by 2.5 for better comparing it with the other spectra.

This means the scattering efficiency and the resonance peaks contrast increase substantially when the cavity is located on the glass substrate. This could be understood by the theory of the virtual mirror image beneath the surface of the substrate.[25, 26] More calculation results for other sizes of silicon SPCs, showing a good agreement between theory and experiment, are plotted in the supporting information (SFig. 1 and SFig. 2). Meanwhile, in the supporting information, the calculated light scattering spectra of p- and s-waves for "a" modes and "b" modes for different diameter silicon SPCs located on a glass substrate are shown. As above discussed, this calculation confirms that for the p-polarized light incidence case, the observed Q of "b" modes is sensitive to the incidence angle of the light, while that of "a" modes is not so sensitive. On the other hand, for the s-polarized light incidence case, the observed Q factor of "a" modes is more sensitive than that of the "b" modes.

Finally, Figure 4 shows the variation of the Q values with the incident angle for $a_{12,5}$ (red curves), $b_{9,4}$ (green curves), and $b_{10,4}$ (blue curves) modes. They are indicated by the same colored arrows in Figure 2 and by dashed lines in Figure 3, SFig1 and SFig 2 respectively. Figure 4a shows the values taken from the theoretical simulations and Figure 4b shows the values taken from the experimental data. The dot-dashed lines in Figure 4a indicate the Q values for the cavities that are free standing in air. We will call them as “ideal Q values” from now on. In general, as deduced from the theoretical simulations [Figure 4(a)], the observed Q values of the three studied modes increase quickly as the incident angle increases from normal incidence, and

they approach more slowly to the ideal Q values at higher angles, near 70º. The experimental Q values [Figure 4(b)] were found to be, in general, only a bit lower than the theoretical ones. See for instance the red curves for mode $a_{12,5}$. This indicates the fabricated cavities have a good quality in terms of spherical geometry and uniformity of the refractive index inside them. The main differences between experiment and theory appear around zero degree incidence for $b_{9,4}$ and $b_{10,4}$ modes. We have attributed these discrepancies to the fact that the incident light is shined on the sample after passing through an objective with certain numerical aperture, thus delivering light at incident angles different from zero. The reason why this happens for these modes and not for the other ones could be attributed to their different electromagnetic field distributions. However, more research would be necessary to clarify this fact.

In conclusion, we have shown that the observed Q of a spherical micrometer sized silicon colloid SPC located on a low refractive index glass substrate is angle dependent and can be easily changed just by changing the incident angle of the light. Note that due to the relationship between the photon lifetime inside the cavity and the Q factor of the cavity mode, the observed effect indicates that the lifetime of the photon trapped inside a 3D silicon colloid SPC vary a lot dependent on the incident direction of the couple photon. Our findings may find applications in angle resolved photon-detectors and micrometric size optoelectronic power sources applications.

Methods

The method to obtain spherical silicon colloid microcavities is based on chemical vapor deposition techniques, where disilane gas (Si_2H_6) at high temperatures decomposes into solid silicon and hydrogen gas by the following chemical reaction: Si_2H_6 (g) = 2Si (s) + $3H_2$ (g).[8] We used a quartz tube as a reactor and introduced disilane gas at a pressure of 30 kPa. The reactor was heated by a tubular oven at 420 °C. Silicon colloids are grown in the gas phase and they fall down onto any substrate, namely a silicon slab. They were detached from the silicon substrate and put on a clean glass substrate by micromanipulation. This glass substrate was placed on a sample holder (able to freely rotate) of a custom-made confocal microscope, which allowed measuring the spectra of the transmitted light. Non-polarized light was shined from the glass substrate to the silicon cavity. In the theoretical simulations, we also assumed (as it appears in the experiment), the incident light impinges from the glass substrate into the silicon cavity. We modified an existing code based on the null-field method with discrete sources[27] to calculate the scattering efficiency of single silicon colloids on a glass substrate at different angles of incidence. The refractive index, n, dispersion for silicon colloids was assumed to be that given by the equation $n=A/\lambda^2+B$ [24], where λ is the wavelength of light, $A=1.686\ x10^5\ nm^2$ and B=3.097.[24] This dispersion gives refractive index values lower than those of bulk silicon that we attributed to the existence of some porosity.

[1] Vahala K. J. Optical microcavities, *Nature* **2003**, *424*, 839.
[2] Unlu M. S.; Strite S. Resonant Cavity Enhanced Photonic Devices. *J. Appl. Phys.* **1995**, *78*, 607.
[3] Akahane Y.; Asano T.; Song B. S.; Noda S. High-Q photonic nanocavity in a

two-dimensional photonic crystal. *Nature* **2003**, *425*, 944.
[4] Gerard J. M.; Barrier D.; Marzin J. U.; Kuszelewicz R.; Manin L.; Costard E.; Thierry-Mieg V.; Rivera T. Quantum boxes as active probes for photonic microstructures: the pillar microcavity case. *Appl. Phys. Lett.* **1996**, *69*, 449.
[5] Gayral B; Gerard J. M.; Lemaitre A.; Dupuis C.; Manin L.; Pelouard J. L. High-Q wet-etched GaAs microdisks containing InAs quantum boxes. *Appl. Phys. Lett.* **1999**, *75*, 1908.
[6] Boriskina S. V. Theoretical prediction of a dramatic Q-factor enhancement and degeneracy removal of whispering gallery modes in symmetrical photonic molecules. *Opt. Lett.* **2006**, *31*, 338.
[7] Shi L.; Tuzer T. U.; Fenollosa R.; Meseguer F. A new dielectric metamaterial building block with a strong magnetic response in the sub-1.5-micrometer region: silicon colloid nanocavities. *Adv. Mater.* **2012**, *24*, 5934.
[8] Fenollosa R.; Meseguer F.; Tymczenko M. Silicon colloids: from microcavities to photonic sponges. *Adv. Mater.* **2008**, *20*, 95.
[9] Xifre-Perez E.; Fenollosa R.; Meseguer F. Low order modes in microcavities based on silicon colloids. *Opt. Express* **2011**, *19*, 3455.
[10] Xifre-Perez E.; Domenech J. D.; Fenollosa R.; Munoz P.; Capmany J.; Meseguer F. All silicon waveguide spherical microcavity coupler device. *Opt. Express* **2011**, *19*, 3185.
[11] Shi L.; Meseguer F. Magnetic interaction in all silicon waveguide spherical coupler device. *Opt. Express* **2012**, *20*, 22616.
[12] Shi L.; Harris J. T.; Fenollosa R.; Rodriguez I.; Lu X.; Korgel B. A.; Meseguer F. Monodisperse silicon nanocavities and photonic crystals with magnetic response in the optical region. *Nat. Commun.* **2013**, *4*, 1904.
[13] Painter O.; Lee R. K.; Scherer A.; Yariv A.; O'Brien J. D.; Dapkus P. D.; Kim I. Two-dimensional photonic band-gap defect mode laser. *Science* **1999**, *284*, 1819.
[14] Tanaka Y.; Upham J.; Nagashima T.; Sugiya T.; Asano T.; Noda S. Dynamic control of the Q factor in a photonic crystal nanocavity. *Nat. Mater.* **2007**, *6*, 862.
[15] Tananbe T.; Notomi M.; Taniyama H.; Kuramochi E. Dynamic release of trapped light from an ultrahigh-Q nanocavity via adiabatic frequency tuning. *Phys. Rev. Lett.* **2009**, *102*, 043907.
[16] Haroche S.; Kleppner D. Cavity quantum electrodynamics. *Physics Today* **1989**, *42*, 24.
[17] Chang R. K.; Campillo A. J. ed., *Optical Processes in Microcavities*, World Scientific, Singapore **1998**.
[18] Chutinan A.; John S. Light trapping and absorption optimization in certain thin-film photonic crystal architectures. *Phys. Rev. A* **2008**, *78*, 023825.
[19] Callahan D. M.; Munday J. N.; Atwater H. A. Solar cell light trapping beyond the ray optic limit. *Nano Lett.* **2012**, *12*, 214
[20] Park Y.; Drouard E.; El Daif O.; Letartre X.; Viktorovitch P.; Fave A.; Kaminski A.; Lemiti M.; Seassal C. Absorption enhancement using photonic crystals for silicon thin film solar cells. *Opt. Express* **2009**, *17*, 14312.
[21] Chen M.; Hu L.; Xu J.; Liao M.; Wu L.; Fang X. ZnO hollow-sphere

nanofilm-based high-preformance and low-cost photodetector. *Small* **2011**, *7*, 2449.
[22] Tian B.; Zheng X.; Kempa T. J.; Fang Y.; Yu N.; Yu G.; Huang J.; Lieber C. M. Coaxial silicon nanowires as solar cells and nanoelectronic power sources. *Nature* **2007**, *449*, 885.
[23] Conwell P. R.; Barber P. W.; Rushforth C. K. Resonant spectra of dielectric spheres. *J. Opt. Soc. Am. A* **1984**, *1*, 62.
[24] Badran R. I.; Al-Hazmi F. S.; Al-Heniti S.; Al-Ghamdi A. A.; Li J.; Xiong S. A study of optical properties of hydrogenated microcrystalline silicon films prepared by plasma enhanced chemical vapor deposition technique at different conditions of excited power and pressure. *Vacuum* **2009**, *83*, 1023.
[25] Albooyeh M.; Simovski C. R. Huge local field enhancement in perfect plasmonic absorbers. *Opt. Express* **2012,** *20*, 21888.
[26] Xifre-Perez E.; Shi L.; Tuzer U.; Fenollosa R.; Ramiro-Manzano F.; Quidant R.; Meseguer F. Mirror-image-induced magnetic modes. *ACS Nano*, **2013**, *7*, 664.
[27] Doicu A.; Wriedt T.; Eremin Y. A. *Light Scattering by Systems of Particles*, Springer Verlag, Berlin **2006**.

Supporting information

Theoretical scattering efficiency simulations and experimental transmission spectra of one 2.546 μm and one 2.348 μm diameter silicon spherical cavities located on a glass substrate.

Acknowledgments

The authors acknowledge financial support from the following projects MAT2012-35040, FIS2009-07812, Consolider 2007-0046 Nanolight, and the PROMETEO/2010/043. L. Shi thanks the financial support from the MICINN (Estancias de profesores e investigadores extranjeros en centros españoles) fellowship program.

Figures and Captions

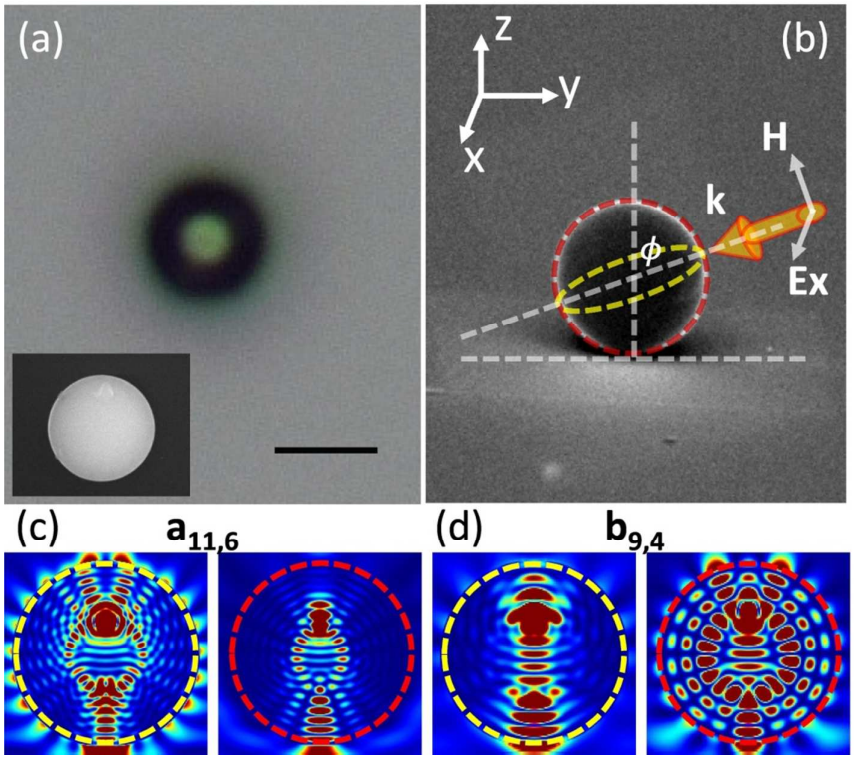

Figure 1. (a) Optical and SEM (inset) images of a typical silicon spherical microcavity. The bar is 3 μm. (b) Schematic view of the microcavity on a glass substrate. The orange arrow indicates the k vector of the incident light, ϕ is the angle between the k wavevector and the z direction. The light is polarized linearly with the electric field, Ex, pointing to the x direction. It defines two planes: one parallel (dash yellow line) and the other one perpendicular (dash red line) to Ex, where "a" and "b" modes occur respectively. (c, d) Electric field distribution of $a_{11,6}$ (c) and $b_{9,4}$ (d) Mie modes in the two perpendicular planes indicated in (b).

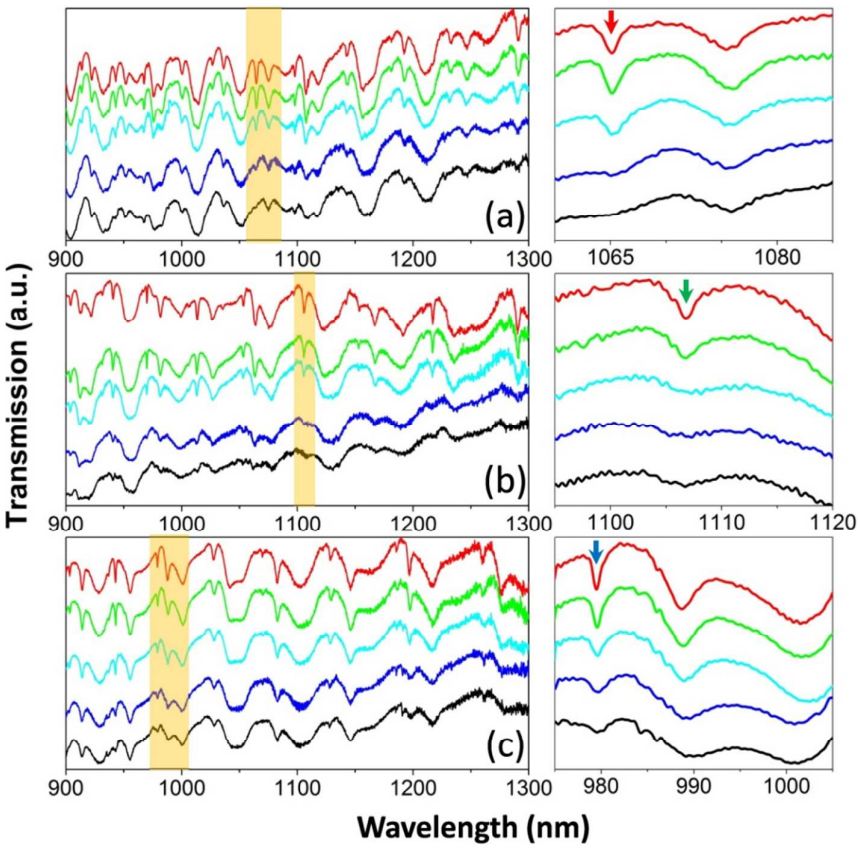

Figure 2. Optical transmission properties of silicon spherical cavities located on a glass substrate for three different diameter values: 3.310 μm (a), 2.546 μm (b) and 2.348 μm (c). The areas highlighted by orange color in the left panels are magnified in the right panels. Black, blue, light blue, green and red color curves correspond to light incident angles of 0º or normal, 20º, 40º, 60º, and 70º. To show clearly all the spectra, they have been shifted vertically to each other. The red, green and blue arrows of the right panels indicate $a_{12,5}$, $b_{9,4}$, and $b_{10,4}$ Mie resonances respectively whose Q variation is analyzed in Figure 4.

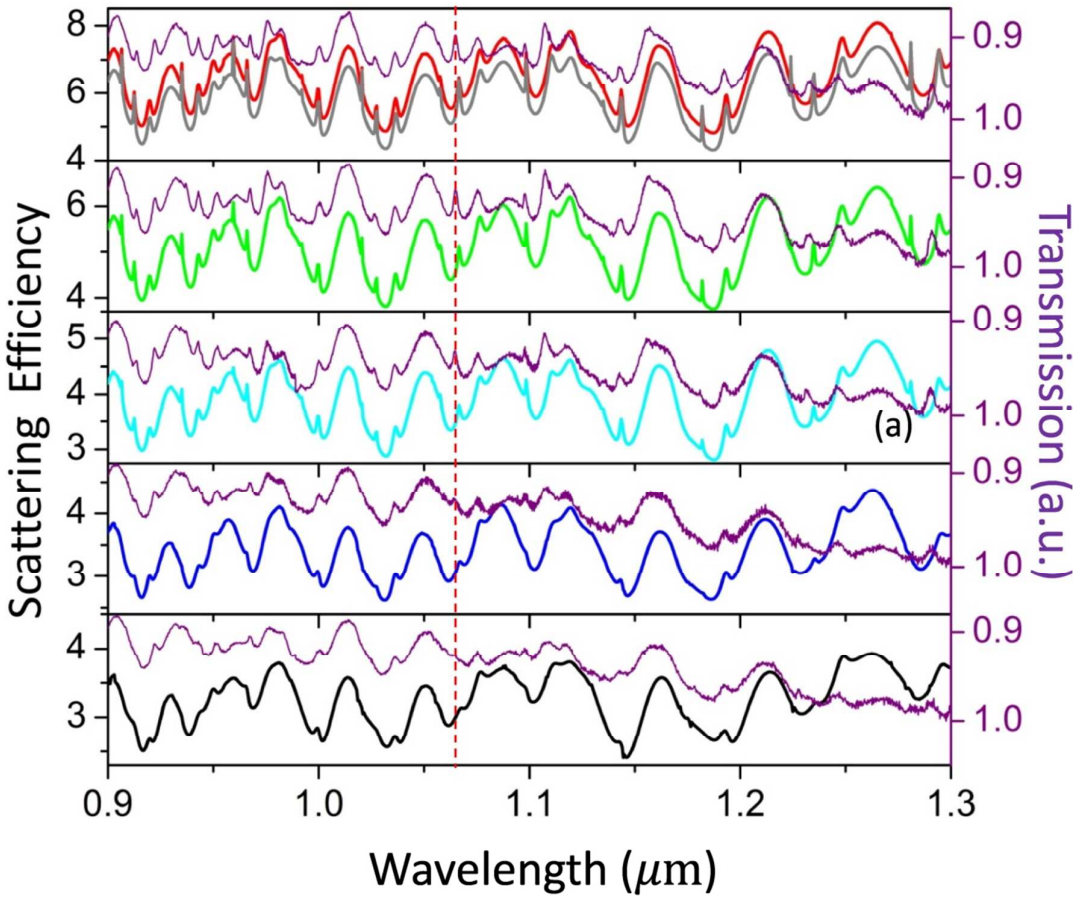

Figure 3. Theoretical simulations of the light scattering on a 3.310 μm diameter silicon spherical cavity located on a glass substrate. (a) Spectra at light incident angles, ϕ, of 0º, 20º, 40º, 60º and 70º are shown by black, blue, light blue, green and red curves respectively in different panels. For comparison, in each panel, the corresponding experimental spectrum is also shown by a purple curve. The grey line in the top panel corresponds to the spectrum of the same cavity free standing in air. This spectrum has been multiplied by 2.5 for a better comparison. The vertical dashed line shows the position of the $a_{12,5}$ mode indicated by a red arrow in figure 2.

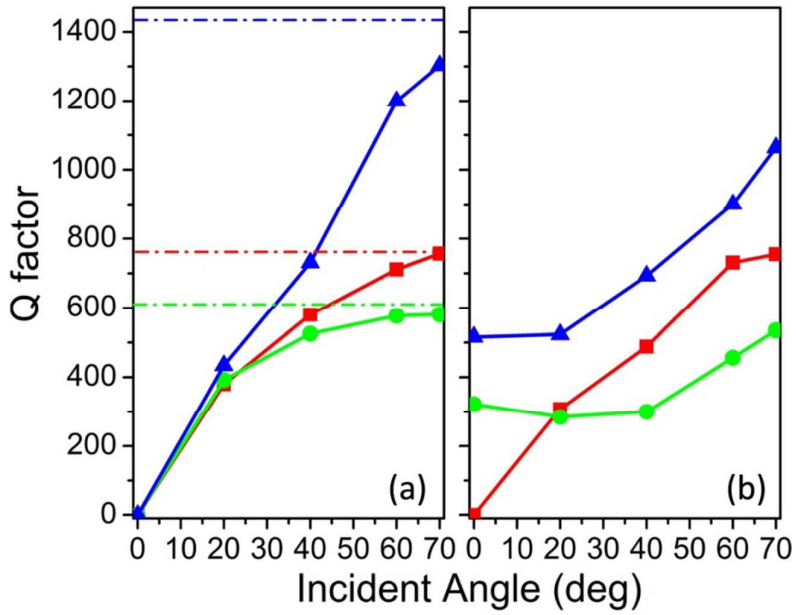

Figure 4. The Quality factor value for silicon colloid spherical microcavities, located on a glass substrate, as a function of the incident angle of light. The symbols in (a) and (b) correspond to the Q values taken from theoretical simulations and from experimental data respectively. Red, green and blue colors correspond to $a_{12,5}$, $b_{9,4}$, $b_{10,4}$ modes respectively, that are indicated by the same color arrows in Figure 2. The solid lines are just linking the symbols. The dash-dot lines indicate the "ideal" Q values for the same cavities when they are free standing in air.

TOC image